

## Ultrafast nonequilibrium spin dynamics in a ferromagnetic thin film

Ganping Ju, A. Vertikov, and A. V. Nurmikko

*Division of Engineering and Department of Physics, Brown University, Providence, Rhode Island 02912*

C. Canady and Gang Xiao

*Department of Physics, Brown University, Providence, Rhode Island 02912*

R. F. C. Farrow and A. Cebollada

*IBM Research Division, Almaden Research Center, 650 Harry Road, San Jose, California 95120-6099*

(Received 20 August 1997)

An ultrafast time-resolved magneto-optical pump probe is applied to study spin-relaxation processes in a ferromagnetic CoPt<sub>3</sub> alloy film. Following spin-selective photoexcitation with circularly polarized femtosecond pulses, transient Kerr ellipticity tracks the evolution of the nonequilibrium spin system. We isolate two distinct processes: a subpicosecond component due to the relaxation of coherently spin polarized electrons, and a slower component ( $\sim 10$  psec) associated with the evolution of the thermalized spin distribution and the photoinduced transient magnetization. [S0163-1829(98)50702-3]

Fast processes associated with changes in the magnetic properties of ferromagnetic media are of both fundamental and applied interest. Experimentally, transient magnetic fields have been applied to switch the magnetization by subnanosecond current pulses in ferromagnetic media.<sup>1</sup> In this case macroscopic constraints on the magnetization vector dominate its dynamics (demagnetization and anisotropy energies). In another limit, photoexcitation of a magnetic medium can create hot, nonequilibrium electrons and spins, so that the magnetic response is modulated at a microscopic level (exchange energy). Quite recently, efforts have emerged that apply ultrafast time-resolved optical techniques to magnetic metals. Vaterlaus *et al.*<sup>2</sup> used time-resolved spin-polarized photoemission to estimate a spin-lattice relaxation time for Gd to be  $\tau \sim 100$  psec, near their experimental resolution. Beaurepaire *et al.*<sup>3</sup> studied the relaxation processes of electrons and their spins in Ni on a picosecond timescale and interpreted their results in terms of an effective temperature model for the coupled spin-electron-lattice system. These experiments are an extension from the study of hot electron dynamics in nonmagnetic metals where an impulse of photoexcitation displaces electrons from equilibrium, and their subsequent relaxation is studied stroboscopically with time-delayed probe pulses. In this manner, information about electron-electron scattering and thermalization,<sup>4</sup> electron-phonon interaction,<sup>5</sup> and hot electron transport has been obtained, typically on simple metals (e.g., Ag, Al, Au).

In the work reported here, we obtain considerable additional insight to the microscopic spin dynamics by ultrafast optical approach by setting up a *selectively* spin-polarized photoexcited gas of electrons in a ferromagnetic metal film on a timescale of  $10^{-13}$  sec. The film possesses perpendicular magnetic anisotropy which facilitates such spin specific excitation, applied at a modest level ( $\sim 10^{18}$  photoelectrons per cm<sup>3</sup>) so that the system overall is weakly perturbed. The transient magneto-optical (MO) response is then recorded via the Kerr ellipticity. As a model system we use the CoPt<sub>3</sub> alloy which has been introduced as a candidate material for

MO recording applications.<sup>6</sup> Two distinct timescales are found to characterize the spin dynamics. On a subpicosecond timescale we measure the relaxation of hot, nonthermal spin polarized (i.e., spin coherent) electrons. The second, slower process involves the equilibration of a thermalized gas of “warm” (disordered) spins and the associated transient magnetization on a timescale of 10 psec.

Either the polar Kerr rotation  $\theta_K$  or the ellipticity  $\epsilon_K$  can be measured to characterize thin MO films with perpendicular magnetization. Both are related to the off-diagonal component of the conductivity tensor  $\sigma_{xy} = \sigma_{1xy} + i\sigma_{2xy}$ , so that  $\epsilon_K \propto C_2\sigma_{1xy} - C_1\sigma_{2xy}$ , while  $\sigma_{xy}$  in turn is proportional to magnetization and the net spin polarization of the medium.<sup>7</sup> For our pump-probe experiments the measurement of transient Kerr ellipticity yields a simpler scheme and a superior detection sensitivity. The experiment employed second harmonic generation from a mode-locked Ti:sapphire laser producing approximately 150 fsec pulses at a repetition rate of 76 MHz at a wavelength of  $\lambda = 435$  nm, chosen to ensure excitation conditions such that  $\hbar\omega \approx 2.85$  eV  $> \Delta_{\text{exch}}$ , the electron exchange energy in CoPt<sub>3</sub>. Quarter waveplates controlled the circular polarization for pump (15 mW) and probe (0.5 mW) beams, focused to a 100  $\mu\text{m}$  spot on the sample, for studying pump induced changes in the reflectivity under the four RCP/LCP pump-probe combinations. The measured changes in the probe reflectance yielded the transient Kerr ellipticity (TEK) from  $\Delta\epsilon_K = (\Delta R/R)_{\text{LCP}} - (\Delta R/R)_{\text{RCP}}$ . A resonant detector with frequency down-conversion lock-in technique<sup>8</sup> allowed us to reach near shot-noise-limit to measure photoinduced changes via TKE for rf amplitude modulated pump beam.

The 20 nm thick CoPt<sub>3</sub> crystalline film was grown by molecular beam epitaxy on a transparent, amorphous substrate (ZrO<sub>2</sub>/glass).<sup>6</sup> The film shows perpendicular magnetic anisotropy with a large Kerr rotation ( $\Theta_K \approx 0.1^\circ$ ), exhibiting nearly 100% remanence with a coercivity  $H_c = 1.6$  kOe and saturation field  $H_s \approx 3.5$  kOe (inset of Fig. 4). For the thin epilayer, the fsec photopumping produces a spatially homogeneous excitation across the film. Figure 1(a) shows the

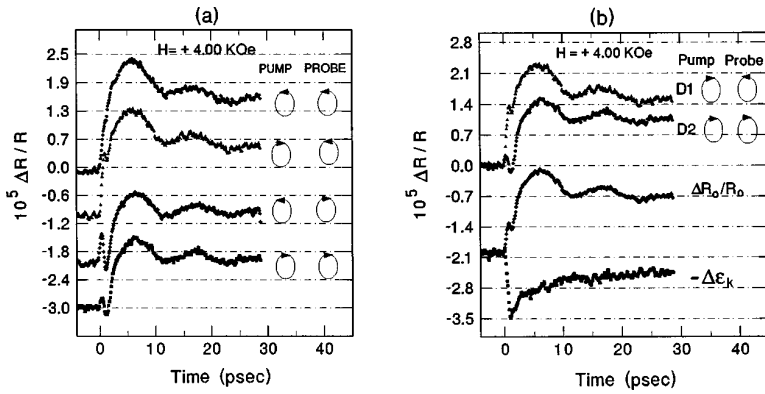


FIG. 1. (a) Transient reflectance at room temperature for different combinations of pump-probe circular polarization in CoPt<sub>3</sub> ( $H = 4$  kOe). The curves are displaced vertically for clarity. (b) The spin-independent [ $\Delta R_0/R_0 = (D_1 + D_2)/2$ ] and spin-dependent components ( $\Delta \epsilon_K = D_1 - D_2$ ).

optically induced transient reflectance,  $\Delta R(t)/R$  in the four pump/probe circular polarizations at room temperature in an external field of  $H = 4$  kOe (i.e., well into saturation). As a check, reversal of the field produces a wholly symmetric set of traces with the LCP/RCP senses reversed. The transient reflectance shows features on a short ( $\sim 1$  psec) timescale which are associated with hot electron/spin phenomena. The slower variations include a large contribution from lattice heating (via the photoelastic effect), following the energy transfer from the hot electrons into the lattice, which results in a transient strain in the CoPt<sub>3</sub> film. Such “picosecond ultrasonic” effects in normal metals have been studied by Chu *et al.*<sup>9</sup> and feature a characteristic oscillation due to multiple reflections of the traveling strain pulse from film/air and film/substrate interfaces. Two cycles of such oscillations can be seen in Fig. 1(a) (the periodicity is related to the ultrasound velocity in CoPt<sub>3</sub>). While the thermoelastic contribution can dominate the photomodulated reflectance for thin metal films, it is insensitive to circular polarization of the probe beam and to an external magnetic field (assuming a negligible magnetostriction) and is easily subtracted out from the data. However, it provides a useful measure of the lattice heating and cooling rates of the CoPt<sub>3</sub> film.

The bottom traces of Fig. 1(b) show how TKE is obtained from the differential reflectivities for opposite circularly polarized probes (at fixed pump polarization):  $\Delta \epsilon_K = (\Delta R/R)_{LCP} - (\Delta R/R)_{RCP}$ . This gives us direct access to the spin (i.e., circular polarization) *independent* contribution can also be obtained from the data as  $\Delta R_0/R_0 = [(\Delta R/R)_{LCP} + (\Delta R/R)_{RCP}]/2$ . Analysis shows that the thermoelastically dominant signal reaches maximum in approximately  $\tau \approx 6$  psec, indicative of the energy transfer rate from the electrons to the lattice (electron-phonon interaction). We also identified a faster, purely electronic optical response ( $\tau \approx 700$  fsec) which corresponds to the initial thermalization time for the hot electron bath.<sup>5</sup> Details of the spin independent hot electron dynamics in CoPt<sub>3</sub> and related alloys will be described elsewhere.

The measured TKE is distinctly dependent on the sense of circular polarization of the pump and also influenced by a magnetic field. The pump polarization dependence is illustrated in the upper traces of Fig. 2 (at  $H = 2.5$  kOe). For further identification of the spin dynamics, it is useful to take both the *average* and the *difference* in the Kerr ellipticity for the RCP and LCP pump excitations, as shown by the lower traces in the figure. We interpret these two contributions as follows. The average (i.e., *pump* polarization independent)

contribution reflects the evolution of the *thermalized* (disordered) spin population expressed as  $\Delta \epsilon_{Kth} = [\Delta \epsilon_K(t)_{RCPpump} + \Delta \epsilon_K(t)_{LCPpump}]/2$ . The difference trace in Fig. 2 yields a direct access to the *nonthermal*, i.e., coherent spins from  $(\Delta \epsilon_K)_{nonth} = [\Delta \epsilon_K(t)_{RCPpump} - \Delta \epsilon_K(t)_{LCPpump}]/2$ . Due to the preferential excitation of majority or minority spins by a circular polarized pump via an electric dipole transition, we create at  $t = 0$  an initial distribution of hot (i.e., nonthermalized) electrons with finite net spin polarization. The difference trace  $(\Delta \epsilon_K)_{nonth}$  in Fig. 2 is proportional to this polarization. The energetic spins thermalize by spin-dependent electron-electron scattering processes, a feature that has not, to our knowledge, been previously directly measured in a magnetic metal. From the data of Fig. 2, the decay time of the nonthermal spin distribution can be obtained:  $\tau_{th} \approx 600$  fs. On the other hand, the risetime of the pump polarization independent trace in the figure correlates with the increase in the effective spin temperature of a thermalized spin distribution:  $\tau_{th} \approx$  of 1.6 ps. This value is distinctly longer than the (spin-independent) electron thermalization time  $\tau_e \sim 700$  fs which we obtain from the “conventional” transient reflectance data. The subsequent decay of  $\Delta \epsilon_{Kth}(t)$ , after the hot electrons have transferred their energy to the lattice, is dominated by the heat transport to the substrate with a decay time of approximately 180 psec. (This process controls the speed of conventional “thermomagnetic” writing in MO recording). Nonetheless, we can extract important information about the spin and transient magnetization relaxation processes, as discussed below. Figure 3 shows the behavior of

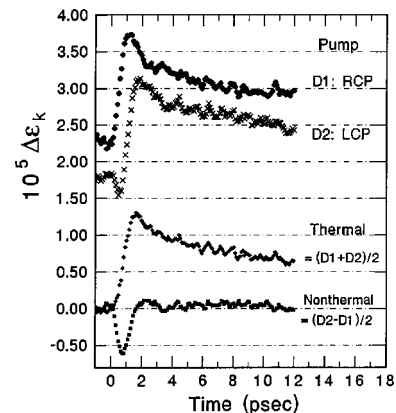


FIG. 2. Dependence of the transient Kerr signal  $\Delta \epsilon_K(t)$  on pump circular polarization (upper traces) and the contributions by thermalized (non-equilibrium) and nonthermal spins (lower traces).

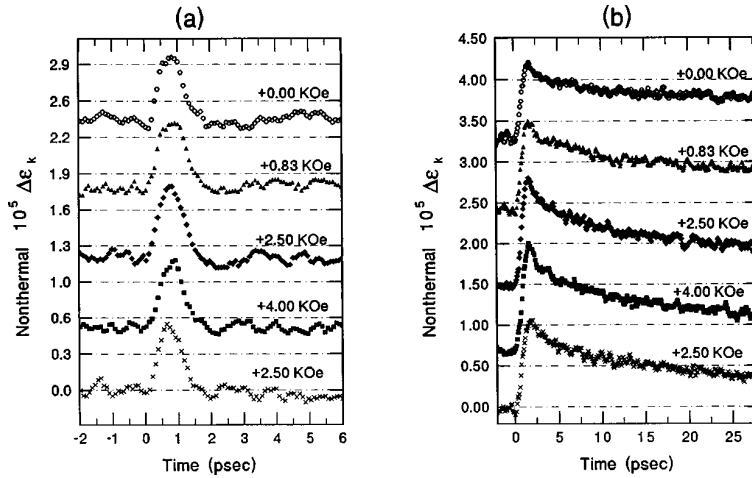


FIG. 3. (a) Transient Kerr signal due to nonthermal spins as a function of magnetic field (from bottom up: first to saturation then to remanence); (b) corresponding data for the thermalized spins.

the thermal and nonthermal components of the TKE for a range of magnetic fields. While the nonthermal component is independent of the field, there is a finite field imprint on the thermalized component.

The physical processes in the data of Figs. 2 and 3 represent complex time-dependent behavior within a nonequilibrium system composed of three coupled degrees of freedom: spin, electron, and lattice. Following the impulse of photoexcitation which creates a nonthermal electron and spin distribution, the electron/spin components thermalize through spin-conserving [at a rate  $\sim 1/(\tau_{\text{th}})^e$ ] and spin-flip scattering processes, respectively. Energy transfer to the lattice is dominated by the electron-phonon interaction (at a rate  $\sim 1/\tau_{\text{el}}$ ), which acquires a subsequent transient temperature increase. In our case, probably not atypical of ferromagnetic metals, the timescales for these processes span a sufficient range so that simplifications can be made in a rate equation approach to model the nonequilibrium system. Guided by insight from the measurements, we distinguish between a short time regime ( $< 1$  psec) where all the excitation remains in the spin and electronic degrees of freedom, and a longer timescale ( $> 1$  psec) where the electron system has thermalized with the lattice (via electron-phonon interaction) and the excited spins and their associated magnetization relax by interacting with this reservoir, as measured by  $\Delta\epsilon_{\text{Kth}}(t)$ .

In the short time regime, defined as  $(\tau_{\text{th}})^e < t < \tau_{\text{el}}$ , the following rate equations are adapted to describe the evolution of the nonthermal spin population  $N_s$ , interacting with the coupled electron and the thermalized spin distributions. We assume that the latter two can be assigned an effective temperature  $T_e$  and  $T_s$ , respectively:

$$\partial N_s / \partial t = -\alpha N_s - \beta N_s, \quad (1a)$$

$$C_s \partial T_s / \partial t = G_{es}(T_e - T_s) + \alpha N_s, \quad (1b)$$

$$C_e \partial T_e / \partial t = -G_{es}(T_e - T_s) + \beta N_s, \quad (1c)$$

The quantity  $\alpha N_s$  describes the heating of the spin gas by the nonthermalized hot spins and  $\beta N_s$  represents the direct coupling of the nonthermal spins and electrons. Under our weak excitation conditions and to keep the problem tractable, the effective temperature concept is a not unreasonable first approximation, given the main thrust of our effort, namely to identify fast spin-dependent processes. The spin dependent

scattering rate  $\beta = G_{es}/C_s$  is proportional to the strength of the electron-spin coupling, with  $C_s$  as the heat capacity of the spin reservoir (the electronic heat capacity is denoted by  $C_e$ ).

For perturbative effective temperature changes ( $\Delta T_e, \Delta T_s \ll T_0$ , the ambient temperature),  $C_e$ ,  $C_s$ , and  $G_{es}$  are approximated as constants and the differential equations are linear. Simultaneous solutions yield the following time dependences for the evolution of the nonthermal and thermalized spins, respectively:

$$N_s \propto H(t) \exp(-t/\tau_{\text{th}}), \quad (2a)$$

$$(T_e - T_s) \propto H(t) [1 - \exp(-t/\tau_{\text{th}})] \exp(-t/\tau_{es}), \quad (2b)$$

where  $H(t)$  is a generalized response function,  $\tau_{\text{th}} = 1/(\alpha + \beta)$ ,  $\tau_{\text{th}} = 1/(\alpha - \beta C_s/C_e) = 1/(\alpha - G_{es}/C_e)$ , and  $\tau_{es} = 1/(\beta + \beta C_s/C_e) = 1/(G_{es}/C_s + G_{es}/C_e)$ . From the data of Figs. 2 and 3(a) we have already identified  $\tau_{\text{th}} \sim 600$  fsec as the decay time of the nonthermal spin distribution. The decay is unsurprisingly independent of the external magnetic field, given the large initial hot electron energies ( $\sim eV$ ). The risetime for the buildup of a thermalized spin distribution, i.e., of  $(T_s - T_e)$ , is measured as  $\tau_{\text{th}} \sim 1.6$  psec from Fig. 3(b). From  $1/\tau_{es} = 1/\tau_{\text{th}} - 1/\tau_{\text{th}}$ , we obtain for the electron-spin relaxation time  $\tau_{es} \sim 1$  ps. The corresponding value for the electron-spin coupling is  $G_{es} \approx 5 \times 10^{17}$  W m $^{-3}$  K $^{-1}$ , measured as an average over a fairly wide energy range ( $\sim eV$ ). The simple model thus reflects an experimental ability to create a short lived coherent spin polarization in the excited states of a ferromagnetic metal. We estimate that the maximum effective spin temperature reached upon spin thermalization is about  $50^\circ$  above the ambient. This compares with the Curie temperature of CoPt $_3$  of  $T_c \approx 500^\circ$  K.<sup>10</sup>

On a longer timescale ( $> 1$  psec), the data of Fig. 3(b) does not readily lend itself for a simple rate equation analysis. This is partly due to the fact that the slow rate of heat transport from the film to the substrate dominates the measured  $\Delta\epsilon_{\text{Kth}}(t)$  and leads to ambiguous fits to experiment from a solution to the coupled differential equations in terms of effective temperatures  $T_s(t)$ ,  $T_e(t)$ , and  $T_l(t)$  (of the lattice). The data does contain a fast component (decay constant  $\approx 6$  psec), which reflects the impact of the electron energy relaxation by phonon emission on the coupled spin-

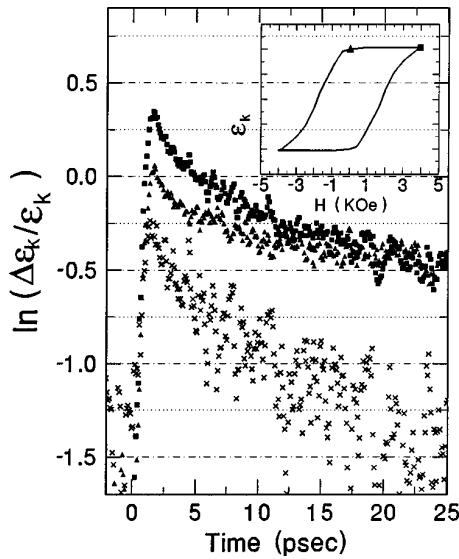


FIG. 4. Normalized transient Kerr signal  $\ln(\Delta\epsilon_K/\epsilon_K)$  at  $H=4$  kOe (closed squares) and  $H=0$  (closed triangles), and their difference (crosses). The inset shows the static Kerr loop for the CoPt<sub>3</sub> film.

electron-phonon system. Beyond this expected time signature, we now focus on the magnetic field dependent features.

It is important to note that at least two distinct contributions to the transient Kerr effect can be expected due to (a) changes in the (spin-dependent) electron occupancy factors in the excited and ground (joint density of) states, and (b) changes in the local magnetization induced by the photoexcited nonequilibrium spins interacting with the ferromagnetic background. This can be seen, for example, by writing the Kerr conductivity as  $\sigma_{xy} \sim \langle s_z \rangle P_0$ , where  $\langle s_z \rangle$  is proportional to the net joint spin polarization in the ground and excited states,  $\langle s_z \rangle \sim (n_{g\uparrow}n_{e\uparrow} - n_{g\downarrow}n_{e\downarrow}) / (n_{g\uparrow}n_{e\uparrow} + n_{g\downarrow}n_{e\downarrow})$ , while  $P_0$  is proportional to the magnetization  $M$  (through the spin-orbit coupling); hence  $\Delta\sigma_{xy}/\sigma_{xy} \sim \Delta\langle s_z \rangle / \langle s_z \rangle + \Delta P_0 / P_0$ . It is reasonable to assume that process (a) dominates the probe response in the measurement of  $(\Delta\epsilon_K)_{\text{nonth}}$  on the subps timescale where photoelectrons are distributed over a wide energy range. We now suggest that an additional finite contribution due to a transient magnetization component, can be extracted from the data such as in Fig. 3(b), once the electrons and spins have thermalized to near  $E_F$ . This is illustrated in Fig. 4 which plots  $\Delta\epsilon_{\text{Kth}}(t, H)/\epsilon(H)$  on a semilogarithmic scale, for external fields at saturation (4.0 kOe) and remanence, as well as their difference. Closer study of the temporal decay of  $\Delta\epsilon_{\text{Kth}}(t, H)/\epsilon(H)$  shows the presence of

three distinct contributions: (1) a transient associated with electron-phonon interaction of approximately 6 psec duration (as already mentioned), (2) a distinctly magnetic field dependent contribution, and (3) the long tail due to heat conduction into the substrate of the fully equilibrated spin/electron/lattice system (as also mentioned). The second contribution is quite intriguing and we conjecture that it represents a transient magnetization effect,  $\Delta M(t) \sim \Delta P_0(t)$ , arising from the interaction of the thermalized spins locally with the ferromagnetic background ( $\Delta M/M_s \ll 1$ ). The differential trace in Fig. 4 isolates this contribution. A possible view emerges from the analog to the magnetic polaron concept in semiconductors where a localized magnetic impurity exchange interacts with band electrons to form a collective local magnetic entity.<sup>11</sup> In the present instance, the photoexcited (though itinerant) spins might assume the role of such impurity moments, assuming that their density and spin diffusion rates are low enough to validate the polaron model. In zero field, the thermalized spins define local axes of the polaron and the contribution to  $\Delta M$  is minimum [in fact, the  $H=0$  Oe trace in Fig. 4 can be fitted with two time constants corresponding to processes (1) and (3) defined above]. The decay of  $\Delta M(H)$  yields a time constant of  $\tau_M \approx 20$  psec, associated with the relaxation of this photoinduced magnetization. On the other hand, a crude estimate for the spin diffusion length gives  $\delta_s = (2DT_2)^{1/2} \sim [2(v_F^2\tau/3)T_2]^{1/2}$  (Ref. 12), where  $v_F$  is the Fermi velocity,  $\tau$  is the Drude-like electron scattering ( $\tau \sim 10^{-13}$  sec), and  $T_2 \sim 20$  psec is the effective spin/magnetization dephasing. We obtain  $\delta_s \sim 1000$  Å which is larger than the estimated average separation of the photoexcited spins under our injection conditions. Hence the polaron picture of isolated local clusters, is probably too simplistic, though possibly useful in capturing the physical idea of photoinduced transient magnetization.

In summary, we have employed a time-resolved optical technique to track nonequilibrium spin dynamics following fsec photoexcitation. We have identified distinct processes in the relaxation of the spin degree of freedom, in particular the existence of a transient spin polarized hot electron gas, and suggested that the thermalized spins contribute to a transient magnetization effect. These types of experiments can be extended to other homogeneous and heterogeneous materials for fundamental study, and can also be useful in the design of fast magneto-electronic devices which selectively exploit the spin degree of freedom.

This work was supported by the National Science Foundation, Grant Nos. DMR91-21747 and DMR97-01579. The authors are grateful to H. Maris for enlightening comments.

<sup>1</sup>For example, W. Doyle *et al.*, IEEE Trans. Magn. **29**, 3634 (1993).

<sup>2</sup>A. Vaterlaus *et al.*, Phys. Rev. B **46**, 5280 (1992).

<sup>3</sup>E. Beaurepaire *et al.*, Phys. Rev. Lett. **76**, 4250 (1996).

<sup>4</sup>C.-K. Sun *et al.*, Phys. Rev. B **50**, 15 337 (1994); W. S. Fann *et al.*, Phys. Rev. Lett. **66**, 2834 (1992).

<sup>5</sup>(a) P. B. Corkum *et al.*, Phys. Rev. Lett. **61**, 2886 (1988); (b) R. Groeveld *et al.*, Phys. Rev. B **45**, 5079 (1992); (c) G. Tas and H. Maris, *ibid.* **49**, 15 046 (1994).

<sup>6</sup>R. F. C. Farrow *et al.*, Mater. Res. Soc. Symp. Proc. **343**, 375 (1994).

<sup>7</sup>For example, W. Reim and J. Schoenes, *Ferromagnetic Materials*, edited

by K. H. J. Buschlow and E. P. Wohlfart (Elsevier, New York, 1990), Chap. 2.

<sup>8</sup>S. Savikhin, Rev. Sci. Instrum. **66**, 4470 (1995).

<sup>9</sup>T. C. Chu *et al.*, Phys. Rev. B **44**, 4281 (1991).

<sup>10</sup>R. F. C. Farrow *et al.*, in *Magnetism and Structure in Systems of Reduced Dimension*, edited by R. Farrow *et al.* (Plenum, New York, 1993), p. 201.

<sup>11</sup>For example, P. A. Wolff, in *Semiconductors and Semimetals*, edited by J. K. Furdyna (Academic, New York, 1987), Vol. 26.

<sup>12</sup>M. Johnson and R. H. Silsbee, Phys. Rev. B **37**, 5312 (1988).